Journal of Materials Chemistry A

Accepted Manuscript

ROYAL SOCIETY OF CHEMISTRY

www.rsc.org/materialsA

Journal of Materials Chemistry A

PAPER

Tuning the catalytic selectivity in biomass-derived succinic acid hydrogenation on FeO_x-modified Pd catalysts†

Xiaoran Liu,‡[ac] Xicheng Wang,‡[a] Guoqiang Xu,[a] Qiang Liu,[ac] Xindong Mu*[a] and Haichao Liu*[b]

Received 00th January 20xx,
Accepted 00th January 20xx

DOI: 10.1039/x0xx00000x

www.rsc.org/

Succinic acid is an important biomass-derived C4 building block and is ready to be converted into various value-added chemicals. Here we report that tunable selectivity for the formation of 1,4-butanediol, γ-butyrolactone and tetrahydrofuran from aqueous succinic acid hydrogenation could be achieved on FeO_x-promoted Pd/C catalysts. Fe was found to be an efficient promoter for the succinic acid hydrogenation, which not only improved the activity of the catalysts but also tuned the product distribution. Succinic acid could be transformed into 1,4-butanediol with a yield of over 70% in the presence of Pd-5FeO_x/C catalyst under the relatively mild conditions of 200°C and 5 MPa H_2. The reaction pathway was also proposed according to the reaction and characterization results.

Introduction

The diminishing fossil resources and the worldwide environmental problems throughout the production of fuels and chemicals impede the development of the chemical industry and motivate researchers to develop environmentally friendly approaches based on sustainable raw materials.[1, 2] Lignocellulosic biomass, which is recognized as the most abundant and viable renewable, has attracted intensive attentions.[3] To date, quite a few chemicals and fuels can be produced from lignocellulose.[4] Succinic acid (SA) which was once synthesized from maleic anhydride, has become economically feasible and commercially available from fermentation.[5, 6] In this process, carbon dioxide which is regarded as the culprit of global warming coupled with renewable biomass is transformed into SA *via* fermentation (Fig. 1). SA was selected as one of the most important building blocks in US Department of Energy's report in 2004.[7] As a new C4 building molecular, SA is considered highly promising for the production of a variety of bulk and fine chemicals. For example, SA could be converted into 1,4-butanediol (BDO), γ-butyrolactone (GBL) and tetrahydrofuran (THF), which are traditionally produced from the maleic anhydride.[8, 9] The catalytic transformation of biomass-derived SA to downstream products will combine the advantages of both bio- and chemo-conversion routes of biomass, and thus has become a topic of worldwide interest.

For the selective catalytic hydrogenation of SA, Ru-, Pd- and Re- based catalysts are the most investigated as monometallic systems.[9] Song et al. found that Pd and Ru were selective for the production of GBL and THF, respectively.[10, 11] A GBL yield of 54% could be obtained at 71% SA conversion over Pd supported on mesoporous alumina xerogel at 260°C and 6 MPa H_2 using 1,4-dioxane as solvent. When Ru-carbon composite was used, THF was obtained dominantly. Especel et al. reported that Pd supported on TiO_2 was efficient in the aqueous SA hydrogenation to GBL.[12] Both the preparation method and Pd dispersion had significant influences on the rate of SA conversion. Luque et al.[13] found that the selectivity to GBL, BDO and THF could be tuned by changing the metal supported on starbon®, a starch derived mesoporous carbonaceous material.

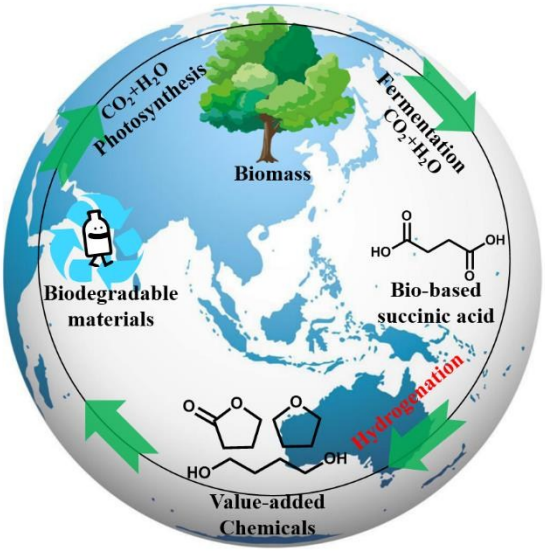

Fig. 1 Carbon cycle of biomass with succinic acid as a building block.

[a] Key Laboratory of Biobased Materials, Qingdao Institute of Bioenergy and Bioprocess Technology, Chinese Academy of Sciences, Qingdao 266101, P. R. China. E-mail: muxd@qibebt.ac.cn
[b] Beijing National Laboratory for Molecular Sciences, College of Chemistry and Molecular Engineering, Peking University, Beijing 100871, P. R. China. E-mail: hcliu@pku.edu.cn
[c] University of Chinese Academy of Sciences, Beijing, 100049, P. R. China.
‡These authors contributed equally to this work.

In order to improve BDO production from SA hydrogenation, bimetallic catalysts, including Ru-Co,[14] Pd-Re[15, 16] and Re-Ru[17] were employed in the SA hydrogenation. Chaudhari et al.[14] found that the activity of SA hydrogenation was greatly improved after the introduction of a small amount of Ru to Co catalyst. The product distribution was modified by impacting the specific hydrogenation steps. Especel et al. studied the aqueous hydrogenation of SA at 160°C under 15 MPa H_2, showing the selective formation of GBL on monometallic Pd-based catalysts.[12, 15, 18] After addition of Re, the bimetallic catalysts Pd-Re/C and Pd-Re/TiO_2 became selective in the BDO formation in one-step SA hydrogenation. Liang et al.[16] found that over the promotion of Re, THF was yielded at an appreciable amount (about 70% yield) over Re-Pd/C catalysts. Mesoporous rhenium-copper-carbon composite, as demonstrated by Song et al, was also effective to modify the product distribution in the SA hydrogenation.[19] Their studies showed that metal particle size of the catalysts was related to the catalytic activity and the yield of GBL and BDO, where smaller average size of metal particle gave a superior hydrogenation activity and higher GBL and BDO yield.

Iron (Fe), a widely distributed transition metal in nature, has been utilized to catalyze various reactions such as ammonia manufacture[20] and Fischer-Tropsch synthesis.[21, 22] However, to the best of our knowledge, no attempt has been reported to adopt Fe as a promoter in the SA hydrogenation. Herein, we reported for the first time that over Pd-FeO_x/C catalysts, GBL, BDO and THF were yielded efficiently via the hydrogenation of SA. The addition of Fe not only enhanced the catalytic activity of SA hydrogenation but also tuned the product distribution. BDO could be obtained at the yield of over 70% with complete conversion of SA over Pd-5FeO_x/C under the condition of 200°C and 5 MPa H_2 in one step.

Experimental Section

Material and catalyst preparation

Palladium chloride was purchased from Sigma Aldrich Chemicals. Hydrochloric acid, nitric acid, SA, GBL, THF and $FeCl_2{\cdot}4H_2O$ were bought from Sinopharm Chemical Reagent Co., Ltd. Biomass-derived SA was provided by C.LAND Science Technology Co., Ltd. The real SA fermentation broth underwent the process of inactivation, filtration and ion exchange, and was then decolorized by active carbon before use. All other reagents were used without further purification.

Commercially available wooden active carbon (denoted as C) was pretreated by 13 wt% HNO_3 at 75°C for 5 h and then washed with deionized water until the filter liquor became neutral. Pd-FeO_x/C catalysts were prepared by the method of incipient-wetness impregnation. In a typical procedure, calculated amount of $PdCl_2$ and $FeCl_2{\cdot}4H_2O$ were first dissolved in appropriate volume of hydrochloric acid solution. The pH of the mixture was adjusted to 4.0 by adding ammonium hydroxide. After that, active carbon was added to the beaker quickly with vigorous agitation. The mixture was sealed and placed at ambient temperature for 24 h before it was dried overnight in a 50°C oven. The catalysts were reduced at 200°C in a pure H_2 flow for 3 h before use. Catalysts were designated as Pd-yFeO_x/C, where y represented the weight percent of the Fe loading, and the content of Pd was fixed at 3 wt%. Monometallic 3 wt% Pd/C and 5 wt% FeO_x/C were also prepared by the same manner.

Catalyst characterization

Temperature-programmed desorption of ammonia (NH_3-TPD) and temperature-programmed reduction in hydrogen (H_2-TPR) of the catalysts were performed using a Micromeritics Autochem 2920 chemisorption analyzer. For the NH_3-TPD characterization, a typical procedure was performed as follows. Firstly, 0.1 g sample was loaded in a quartz U-tube and degassed at 150°C for 2 h. After the adsorption of ammonia at 100°C for 2 h, the sample was then heated to 800°C at the rate of 10 °C/min. For the H_2-TPR analysis, 0.1 g as-prepared catalyst was loaded in a quartz U-tube and degassed at 150°C for 2 h, and then reduced under the H_2 flow at the rate of 10 °C/min. NH_3 and H_2 were detected by a TCD analyzer.

The X-ray powder diffraction (XRD) patterns of the Pd-FeO_x/C catalysts were obtained from a Bruker D8 advance X-ray diffraction meter under Cu-Kα radiation. Transmission electron microscopy (TEM) images, Scanning transmission electron microscopy (STEM) images and STEM element mapping were acquired on a Tecnai G2 F20 S-TWIN transmission electron microscope operated at 200 kV. Nitrogen adsorption-desorption experiments were conducted on a Micromeritics ASAP 2020 static volumetric sorption analyzer. The calculation of the surface area was based on the Brunauer-Emmett-Teller (BET) method. The X-ray photoelectron spectroscopy (XPS) analyses of Pd-FeO_x/C catalysts were conducted in Thermo ESCALAB 250 Xi with Al Kα source (hv = 1486.6 eV; 500 μm spot size) radiation for spectra excitation. The binding energy of peaks was corrected by referencing to the C 1s peak at 284.8 eV. Inductively coupled plasma atomic emission spectroscopy (ICP-AES) experiments were carried out on a Thermo IRIS Intrepid II XSP atomic emission spectrometer to determine the metal leaching after reaction.

Catalytic hydrogenation experiment

Hydrogenation of SA was conducted in a batch system using a 50 mL stainless steel autoclave equipped with magneton stirring. In a typical experiment, 20 mL 1 wt% SA solution and 0.09 g catalyst were loaded into the autoclave. The autoclave was then sealed and purged five times with H_2 to remove air, and pressurized to 5 MPa H_2 at room temperature (RT) and finally programmed to desired temperature under vigorous stirring. The products were identified by gas chromatograph (GC, 7890A, Agilent, USA) coupled with a mass spectrometer (MS, 5975C, Agilent, USA) using a HP-INNOWax column (30 m × 0.25 mm; film thickness, 0.25 μm). Quantification was performed on both by high-performance liquid chromatograph (HPLC) and GC. Unconverted SA was analyzed by HPLC (Waters 1525) equipped with UV and evaporative light scattering (ELS) detectors. The separation was carried out on an Aminex HPX-87H column (300 mm × 7.8 mm) at 35°C. The eluent flow rate was 0.5 mL/min, eluted with 5 mmol/L H_2SO_4 solution. The products were

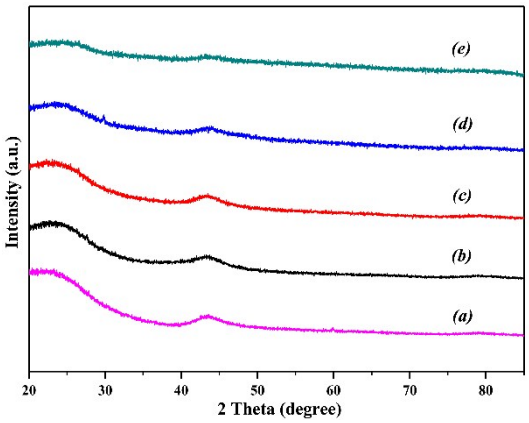

Fig. 2 XRD patterns of the Pd-FeO_x/C catalysts. (a) Active carbon, (b) Pd/C, (c) Pd-1FeO_x/C, (d) Pd-5FeO_x/C and (e) Pd-10FeO_x/C.

quantified on a Varian 450-GC equipped with an FID detector using HP-FFAP column (30 m × 0.25 mm, 0.25 μm phase thickness). Nitrogen was used as the carrier gas at 1 mL/min and the column temperature was from 50°C (2 min) to 240°C (5 min) at a rate of 20 °C/min. The injector and detector temperatures were 250°C and 280°C, respectively.

Results and discussion

XRD patterns of the Pd-FeO_x/C catalysts are shown in Fig. 2 along with the pattern of active carbon for comparison. It can be seen from Fig. 2 that no obvious differences could be distinguished between Pd-FeO_x/C catalysts and active carbon, which indicated that both Pd and FeO_x were well dispersed on the active carbon. TEM images (Figs. 3 and S1) further confirmed that small and dispersed metal particles were presented in the catalysts. It could be observed from the TEM images that mean size of the metal particles (both FeO_x and Pd) increased with increasing the Fe content. As for the Pd/C catalyst, the mean size of the metal particle was found to be 3.7 nm. The metal particle size increased to 4.1 nm in Pd-1FeO_x/C and further increased to 4.4 nm when the Fe loading was 5 wt%. In Pd-10FeO_x/C, the metal particle grew to 7.6 nm. These results are similar with some reports. [23, 24] STEM and STEM element mapping images are shown in Fig. 4. In these images, red and green correspond to Fe and Pd, respectively. It was noticed that both Pd and Fe elements are well dispersed on the support with some agglomerates. Both the elements of Pd and Fe exist in most of the metal particles, indicating that the elements Fe and Pd were contained in the metal particles. The increase of metal

Table 1 The physical and chemical properties of the Pd-FeO_x/C catalysts

Catalysts	Ps[a] (nm)	S_{BET}[b] (m^2/g)	Pore volume (cm^3/g)		Acidity[e] (mol/g)	Pd state in Pd $3d_{5/2}$ (%)	
			V_{micro}[c]	V_{meso}[d]		Pd^0	Pd^{2+}
Pd/C	3.7	1345	0.443	0.317	0.09	60.4	39.6
Pd-1FeO_x/C	4.1	1277	0.416	0.333	0.66	31.4	68.6
Pd-5FeO_x/C	4.4	1001	0.323	0.267	1.18	28.0	72.0
Pd-10FeO_x/C	7.6	828	0.264	0.220	1.88	21.6	78.4

[a] Mean particle size calculated from TEM images. [b] Surface area based on BET method. [c] Micropore volume based on DFT method. [d] Mesopore volume based on DFT method. [e] Data obtained from NH_3-TPD characterization.

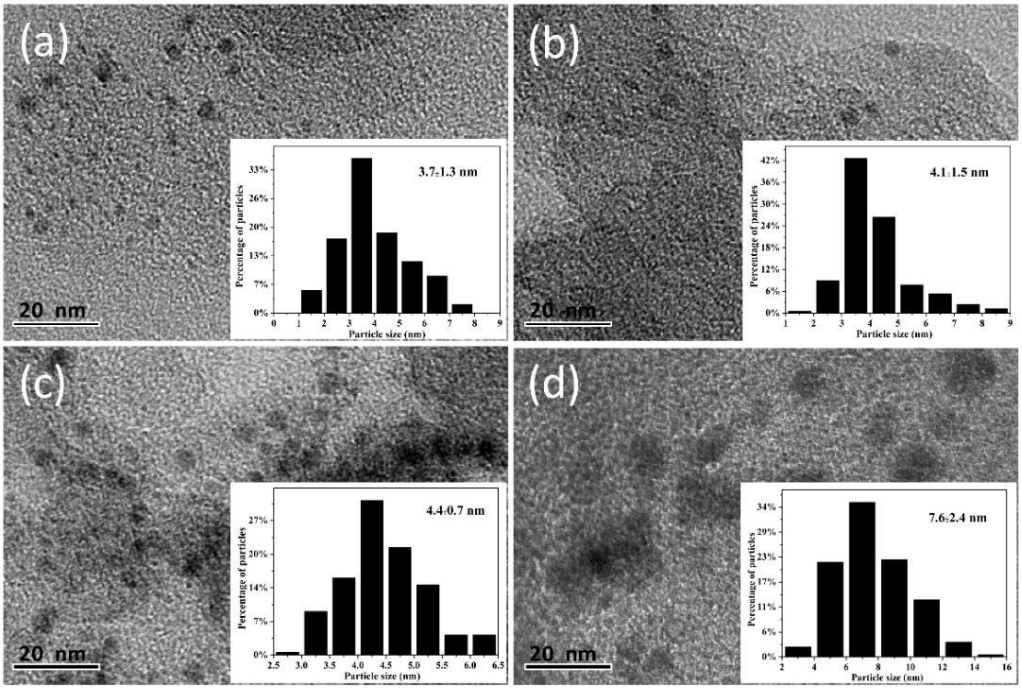

Fig. 3 TEM images of the Pd-FeO_x/C catalysts. (a) Pd/C, (b) Pd-1FeO_x/C, (c) Pd-5FeO_x/C and (d) Pd-10FeO_x/C.

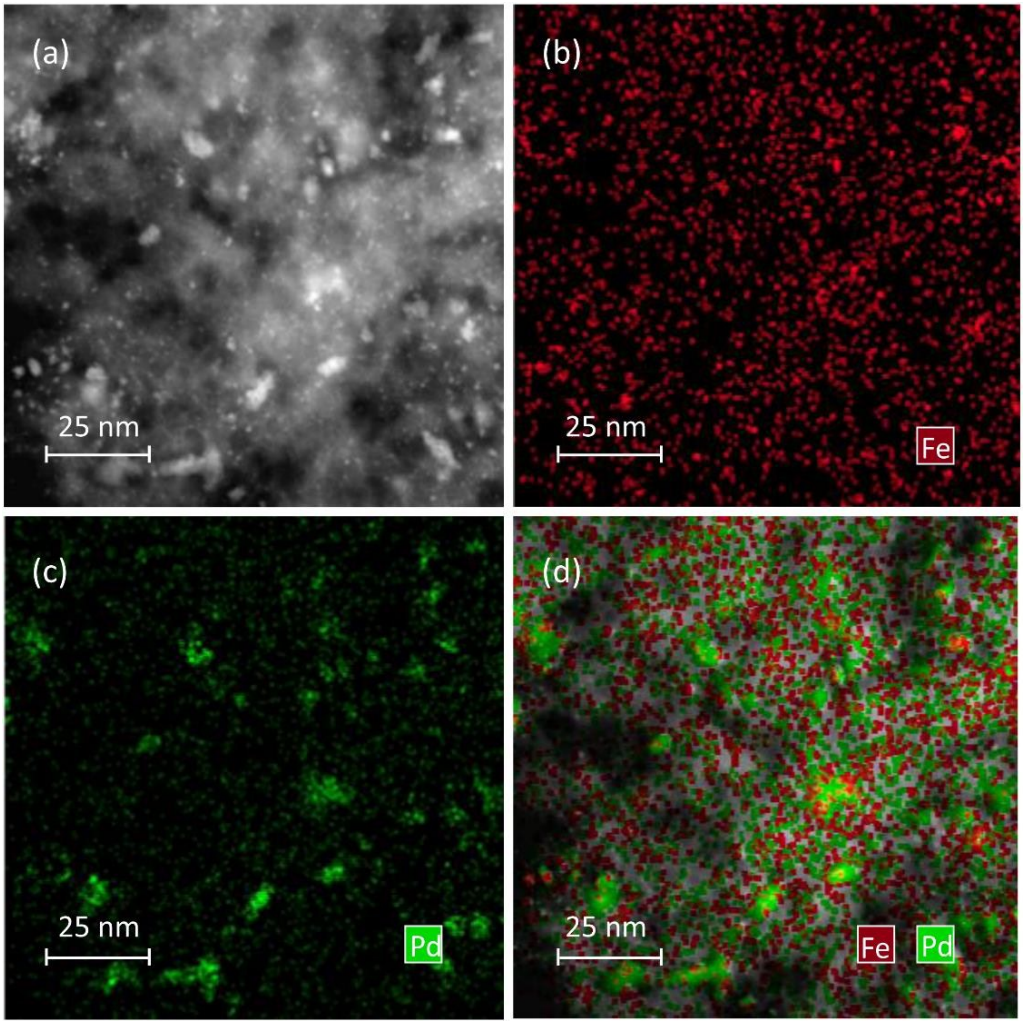

Fig. 4 STEM image (a) and STEM element mapping (b), (c) and (d) of Pd-5FeOx/C.

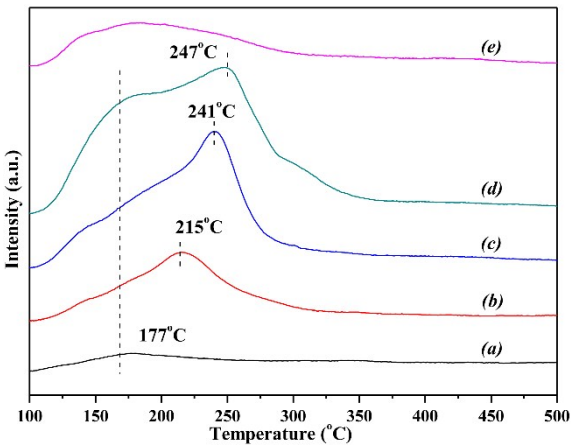

Fig. 5 NH_3-TPD profiles of the Pd-FeO_x/C catalysts. (a) Pd/C, (b) Pd-1FeO_x/C, (c) Pd-5FeO_x/C, (d) Pd-10FeO_x/C and (e) 5FeO_x/C.

particle size might be ascribed to the aggregation of two kinds of metal.

Physical and chemical properties of the catalysts, including the metal particle size, acidity of the catalysts, surface areas, pore volumes and results of XPS analyses, were summarized in Table 1. As shown in Table 1, surface areas and micropore volumes of Pd-FeO_x/C catalysts decreased with the increase of Fe content. Moreover, the mesopore volumes increased first and then decreased with the introduction of FeO_x species. The existence of void space formed among the stacked nano-crystals might explain changes in mesopore volumes.[25] The addition of FeO_x species to the Pd catalysts led to a decrease in surface area and cumulative pore volume, which could be explained by the partial blockage of porous framework of C support by FeO_x species.

Acidity of the catalyst was one of the significant aspects in SA hydrogenation because the intramolecular dehydration was catalyzed by the acidic sites.[11] Consequently, higher acidity of the catalysts led to better activity and superior GBL yield. Therefore, NH_3-TPD analysis was conducted to evaluate the acidity of the prepared Pd-FeO_x/C catalysts. Fig. 5 shows the NH_3-TPD results of the Pd-FeO_x/C catalysts. Pd/C catalyst possessed a low-temperature NH_3 desorption peak at 177°C which was ascribed to weak acid sites and became more intense with increasing the Fe content to 10 wt% on Pd-10FeO_x/C catalysts. Meanwhile, after the addition of Fe, a shoulder peak appeared at higher temperature and migrated to higher temperature (247°C) with the increase of Fe content. These results indicated the presence of new acid sites, and these acid

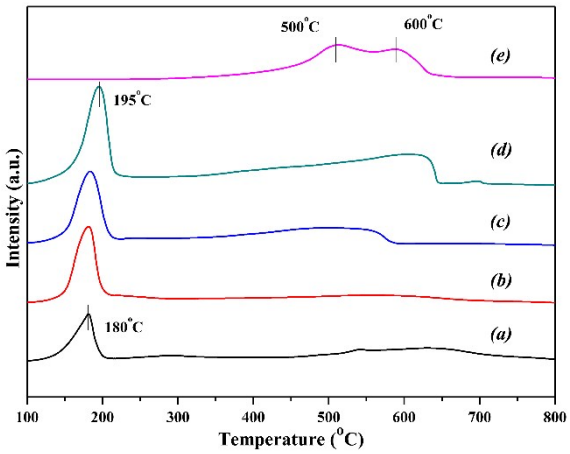

Fig. 6 H_2-TPR profiles of Pd-FeO_x/C with different Fe content. (a) Pd/C, (b) Pd-1FeO_x/C, (c) Pd-5FeO_x/C, (d) Pd-10FeO_x/C and (e) 5FeO_x/C.

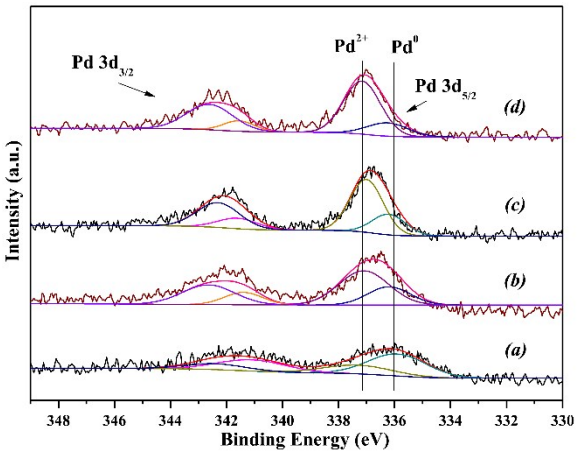

Fig. 7 XPS spectra (Pd 3d) for Pd-FeO_x/C catalysts. (a) Pd/C, (b) Pd-1FeO_x/C, (c) Pd-5FeO_x/C and (d) Pd-10FeO_x/C.

sites became stronger with the increase of the Fe content which might result from the interaction of Pd and FeO_x species. [26, 27]The amount of the acid sites of the catalysts increased from 0.09 mmol NH_3/g on Pd/C to 1.88 mmol NH_3/g with the increase of the Fe content to 10 wt% on Pd-10FeO_x/C (Table 1). Such increase in the acidity might be explained by the generation of more Lewis acid sites at the higher Fe contents.[28, 29]

Fig. 6 demonstrated the H_2-TPR results of as-prepared Pd-FeO_x/C catalysts with different Fe contents. Peaks at about 180°C in the TPR profiles of Pd/C, Pd-1FeO_x/C, Pd-5FeO_x/C and Pd-10FeO_x/C belonged to the H_2 consumed by Pd oxide reduction. The weak peak appeared at 500 - 700°C in the TPR profile of Pd/C was attributed to the reduction of the surface acidic functional groups of the active carbon.[16] However, after Fe was introduced into the Pd/C catalyst, the peak of Pd-1FeO_x/C flattened, indicating that there existed an interaction between Fe and active carbon. The two peaks emerged in the TPR profile of 5FeO_x/C at 500°C and 600°C were attributed to the H_2 consumption of Fe^{3+} and Fe^{2+} reduction, respectively.[30] Nevertheless, as for the Pd-FeO_x/C catalysts, only one peak was observed between 400 - 600°C in the TPR profiles, suggesting that the presence of Pd accelerated the reduction of Fe oxide. On the other hand, the reduction temperature of Pd oxide altered slightly to higher temperature after the addition of Fe (from 180 - 195°C), showing that the existence of Fe prevents the reduction of PdO_x. Such mutual effects denoted the presence of interaction between FeO_x and Pd species in Pd-FeO_x/C catalysts.[30]

In order to acquire the electronic properties of Pd-FeO_x/C catalysts, XPS analysis was employed. Fig. S4 presented the typical C 1s and Fe 2p spectra and no obvious variations in C 1s and Fe 2p binding energy could be observed for the different Pd-FeOx/C catalysts. The enhancement of Fe 2p peak intensity was ascribed to the increase of Fe content in the different catalysts.[31] As shown in Fig. 7, the parent peak of Pd $3d_{5/2}$ in Pd/C located at about 336.2 eV, however, this peak shifted to higher binding energy (from 336.2 eV to 337.2 eV) at higher Fe contents in the Pd-FeO_x/C catalysts. This result suggested that there may exist some variations in Pd chemical states. Therefore, the Pd $3d_{5/2}$ signal was deconvoluted and two pairs of doublets were identified. The peak at about 336.1 eV belonged to metallic Pd. The observed binding energy of Pd 3d was found to be higher than that in the previous reports,[32] which might be ascribed to a strong interaction between Pd and the active carbon support.[13] The peak at about 337.1 eV could be allocated to Pd^{2+}.[33] The contribution of metallic Pd is higher than Pd^{2+} in Pd/C (60.4% vs. 39.6%). The existence of Pd^{2+} state in the reduced Pd/C catalyst was attributed to the contact with air as the sample was moved to the XPS chamber.[34]

However, when Fe was introduced to the catalyst, the percentage of Pd^{2+} increased to 68.6% as the proportion of Pd^0 diminished to 31.4% in Pd-1FeO_x/C. Such changes in the ratio of Pd^{2+} to Pd^0 may be attributed to the interaction between Fe and Pd. The existence of Fe in the catalysts rendered the reduction of Pd oxide more difficult in Pd-FeO_x/C catalysts than in monometallic Pd/C catalyst, which coincides with the H_2-TPR results in Fig. 6, where the reduction temperature of palladium increased to higher temperature when Fe was introduced into Pd/C. When Fe loading was raised to 5 wt%, the ratio of Pd^{2+}/Pd^0 didn't change significantly compared to Pd-1FeO_x/C. It was found that 72.0% of the Pd species was in Pd^{2+} and 28.0% existed in metallic state in Pd-5FeO_x/C. The ratio of Pd^{2+}/Pd^0 was about 3.6 as the content of Fe was further increased to 10 wt%, quite similar to that of the Pd-5FeO_x/C catalyst (Table 1). In a word, the presence of FeO_x in Pd-FeO_x/C catalysts interacted with Pd and thus changed the ratio of Pd^{2+} to Pd^0 in the catalysts. The XPS results provided another evidence for the interaction between FeO_x and Pd.

Fig. 8 demonstrates the results of SA hydrogenation over Pd-FeO_x/C catalysts with different Fe loadings at 5 MPa H_2 and 200°C. Over Pd/C, the conversion of SA was 49.6%. With the promotion of Fe, SA conversion increased notably to 81.9% and 87.7% over Pd-1FeO_x/C and Pd-5FeO_x/C, respectively. Nevertheless, the conversion dropped to 24.6% over Pd-10FeO_x/C. The conversion of SA over Pd-FeO_x/C was first increased and then decreased with respect to the Fe content (Fig. 8). According to the NH_3-TPD results, the addition of Fe

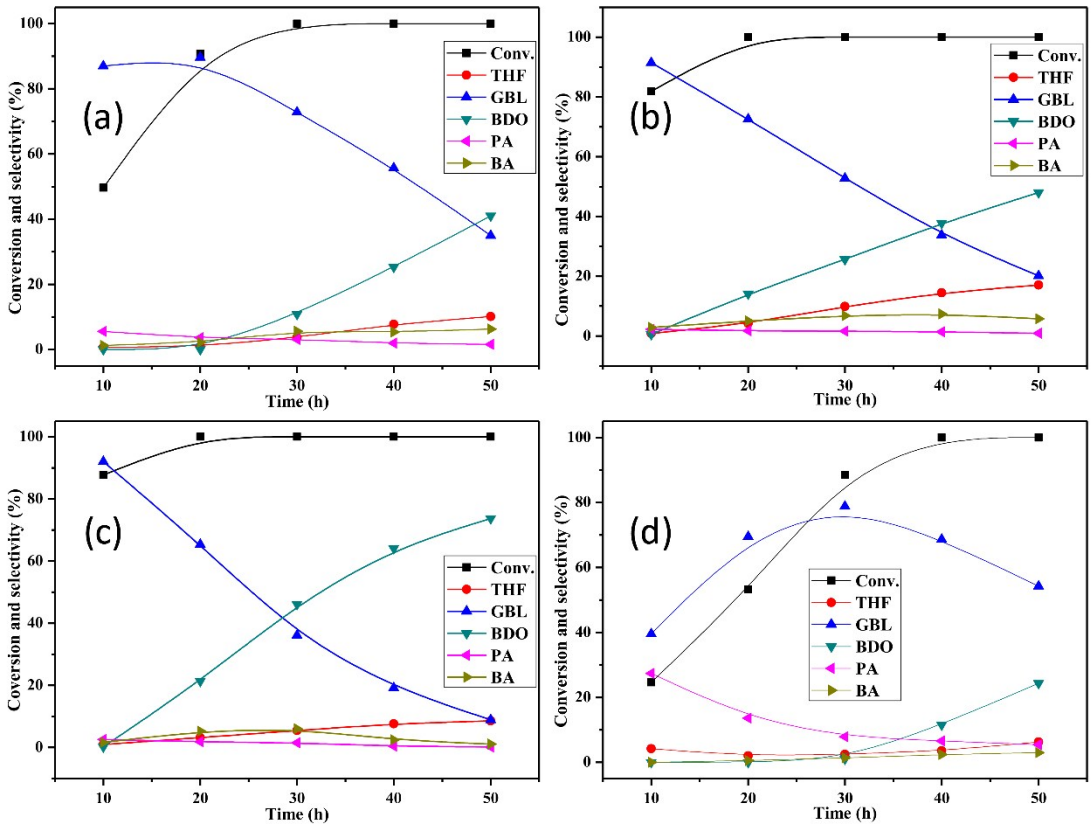

Fig. 8 SA conversion and products selectivities over Pd-FeO_x/C as a function of time at 5 MPa H_2 and 200°C. (a) Pd/C, (b) Pd-1FeO_x/C, (c) Pd-5FeO_x/C and (d) Pd-10FeO_x/C. Conv.: conversion, THF: tetrahydrofuran, GBL: γ-butyrolactone, BDO: 1,4-butanediol, PA: propionic acid and BA: butyric acid.

Table 2 Reaction results of various substrates hydrogenation over Pd-FeO_x/C catalysts[a]

Entry	Substrates	Catalysts	Conv. (%)	Selectivity (%)					
				THF	GBL	BDO	PA	BA	BuOH
1	SA	5FeO_x/C	10.5	0	0	0	0	0	0
2	SA	5FeO_x/C + Pd/C	82.3	1.3	87.4	0	4.6	1.4	0
3	GBL	Pd-5FeO_x/C	76.4	15.5	-	70.8	0	4.0	9.7
4	GBL	Pd/C	25.1	17.5	-	76.2	0	6.3	0
5	GBL	5FeO_x/C	6.6	0	-	0	0	0	0
6	THF	Pd-5FeO_x/C	9.6	-	0	55.2	0	0	44.8
7	BDO	Pd-5FeO_x/C	7.2	89.3	0	-	0	0	10.7

[a] Reaction conditions: T = 200°C; P = 5 MPa H_2 (RT); reaction time = 20 h.

Conv.: conversion, SA: succinic acid, THF: tetrahydrofuran, GBL: γ-butyrolactone, BDO: 1,4-butanediol, PA: propionic acid BA: butyric acid and BuOH: n-butanol.

improved the acidity of the catalysts (Fig. 5). Higher acidity led to better SA conversion as concluded from the results of Pd/C, Pd-1FeO_x/C and Pd-5FeO_x/C, which is in accordance with the results reported by Song et al.[11] Interestingly, SA conversion over Pd-10FeO_x/C which possessed the highest acidity was much lower than the other catalysts, even lower than Pd/C with an acidity of 0.09 mmol NH_3/g. These results indicated that activity of SA hydrogenation must be impacted by other factors. The introduction Fe not only increased the Lewis acid sites of the catalysts which led to higher acidity and better dehydration activity but also accelerated the encapsulation of Pd particles, resulting in bigger metal particles. Higher metal dispersion meant superior accessibility of the active metal sites to hydrogen and reactant and thus led to better SA hydrogenation activity, as found by Especel et al.[12] As shown in Table 1 and Fig. 3, metal particle size of the supported Pd-FeO_x/C catalysts increased with the addition of Fe. The mean particle size of the Pd-1FeO_x/C was about 4.1 nm, larger than that in Pd/C, although the acidity of Pd-1FeO_x/C was 6 times higher than that of Pd/C (Table 1). The SA hydrogenation was controlled by the coordination of both acidity of the catalysts and the dispersion of the active metal. Pd-1FeO_x/C, which possessed higher acidity

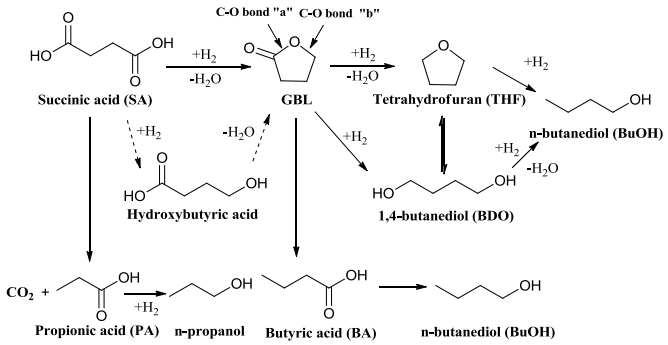

Scheme 1 Reaction pathways of SA hydrogenation over Pd-FeO_x/C.

and slightly bigger metal particle size, gave a much higher SA conversion compared to the Pd/C catalyst.

For the Pd-5FeO_x/C catalyst, the mean particle size was 4.4 nm while the acidity of the catalyst was 1.18 mmol NH_3/g. A relatively higher acidity and the similar mean particle size resulted in a higher SA hydrogenation conversion compared to Pd-1FeO_x/C catalyst (87.7% vs. 81.9%). For the catalyst of Pd-10FeO_x/C, which has a much bigger mean particle size and a relatively higher acidity (1.88 mmol NH_3/g), its SA conversion was as low as 24.6% under the same reaction conditions. These results clearly show that the activity of SA hydrogenation depends on both acidity of the Pd-FeO_x/C catalysts and their Pd dispersion.

Apart from the SA conversion, selectivities to the hydrogenation products were also changed with the increasing of the Fe loading. As shown in Fig. 8, over the monometallic Pd/C catalyst, GBL was produced as the main product together with the formation of THF, propionic acid (PA) and butyric acid (BA) yielded as the by-products, and no BDO was observed after reaction for 20 h. The selectivities to BDO and THF increased slightly while the selectivity to GBL decreased by prolonging the reaction time. This phenomenon presented that BDO and THF were formed from the subsequent hydrogenolysis of GBL. This is in accordance with Chaudhari et al.[14] who proposed that GBL and BDO were formed successively.

Over Pd-1FeO_x/C, BDO was generated with a selectivity of 14.1% after 20 h, and the selectivity to BDO was enhanced to 48.0% when the reaction time was prolonged to 50 h (Fig. 8). At the same time, the selectivity to GBL decreased markedly from 72.6% to 20.1% while the selectivity to THF increased from 4.2 to 17.0%. Moreover, BDO was produced with a selectivity of 70% over Pd-5FeO_x/C under the condition of 200°C, 5 MPa H_2 and 50 h. This result indicated that the addition of non-precious Fe in Pd/C affected both the hydrogenation activity and the product distribution by accelerating the reaction rate of SA hydrogenation to GBL and the subsequent GBL hydrogenolysis to THF and BDO.

In order to clarify whether there existed an interaction between Fe and Pd in Pd-FeO_x/C, the catalytic performances of 5FeO_x/C catalyst and the physical mixture of Pd/C and 5FeO_x/C were compared in the SA hydrogenation (Table 2, Entries 1 and 2). SA could not be converted into GBL, BDO and THF when only 5FeO_x/C was employed. Over the mixture of 5FeO_x/C and Pd/C, both the SA conversion and product distribution were similar to the results over Pd/C, which was inferior to the Pd-5FeO_x/C catalyst. These findings indicated that the close contact between Pd and Fe species is necessary to obtain excellent hydrogenation performance of Pd-FeO_x/C in the selective hydrogenation of SA to BDO, GBL and THF. Therefore, we believe that the superior catalytic performance of Pd-FeO_x/C catalysts in SA hydrogenation may be attributed to the synergy between Pd and Fe species.

In order to figure out the roles of FeOx in the step of SA hydrogenation to GBL and further conversion to BDO, hydrogenolysis of GBL over Pd-FeO_x/C catalysts was conducted. Under the same reaction conditions (200 °C, 5 MPa H_2 and 20 h), as presented in Table 2, over monometallic Pd/C catalyst, BDO as the major product together with THF and BA could be yielded with a GBL conversion of 25.1% (Table 2, entry 4), whereas a GBL conversion of 76.4% could be achieved with comparable product selectivities over Pd-5FeO_x/C(Table 2, entry 3), indicating that the presence of FeO_x species could also promote the step of GBL hydrogenolysis to BDO. Due to the superior performance in both the step of SA hydrogenation to GBL and the subsequent GBL hydrogenolysis to BDO, a higher yield of BDO could be obtained over Pd-5FeO_x/C catalyst.

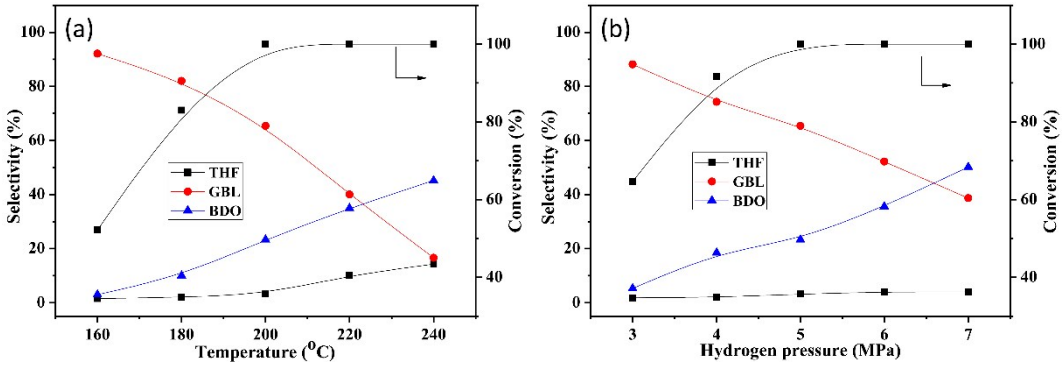

Fig. 9 Hydrogenation of SA over Pd-5FeO_x/C at different (a) reaction temperature and (b) hydrogen pressure. Reaction conditions in (a): 5 MPa H_2, n_{SA}: n_{Pd} = 67:1, 20 h. Reaction conditions in (b): 473 K, n_{SA}: n_{Pd} = 67:1, 20 h. THF: tetrahydrofuran, GBL: γ-butyrolactone, BDO: 1,4-butanediol.

Furthermore, PA, which was observed in SA hydrogenation results, could not be detected in GBL, THF and BDO hydrogenation products (Table 2), indicating that PA was produced directly from SA *via* decarboxylation. The performance of Pd-10FeO_x/C with lower SA conversion but higher PA selectivity (Fig. 8, d) could be interpreted by the decarboxylation over larger metal particles, due to its poor hydrogenation activity, showing that SA was more likely to be converted into PA rather than GBL. GBL was unable to be transformed into THF, BDO and BA over monometallic 5FeO_x/C catalyst under the same reaction conditions (Table 2, entry 5).Over Pd-5FeO_x/C, only a small amount of THF and BDO were converted under the same reaction conditions (Table 2, entry 6 - 7). Consequently, a possible reaction pathway was proposed in Scheme 1, based on the results of Fig. 8 and Table 2. When one carboxyl group in SA was hydrogenated, the formed 4-hydroxybutyric acid was converted to GBL *via* fast intramolecular dehydration. GBL then underwent a ring-opening reaction *via* two different ways. BDO could be obtained if the C-O bond "a" was disrupted, on the other hand, the cleavage of C-O bond "b" brought about the production of BA. THF could also be produced from GBL. At the same time, SA was converted to PA *via* decarboxylation.

We further studied the effect of reaction temperature on the hydrogenation of SA at 5 MPa H_2 over Pd-5FeO_x/C (Fig. 9). SA could also be converted at lower temperature, and GBL was formed as the major product with a small amount of BDO and THF. With elevating reaction temperature, SA conversion increased rapidly with concurrent decrease of selectivity to GBL and increase of selectivity to BDO and THF. Besides, Selectivity to GBL decreased from 92% to 16% whereas selectivity to BDO increased from 3% to 45% as the reaction temperature elevated from 160 to 240°C, reflecting that hydrogenolysis of GBL could also be accelerated at higher temperature. Selectivity to THF increased apparently from 2% to 14% in the range of 160 - 240°C, indicating that higher temperature also promoted the process of GBL to THF, similar to the results reported by Cao et al. [35] in γ-valerolactone hydrogenolysis. However, higher reaction temperature also resulted in the decline of total product selectivity, indicating the further degradation of the products.

Meanwhile, the effect of the hydrogen pressure on the SA conversion and product selectivity at 200°C was also examined. SA conversion increased as the hydrogen pressure increased. Selectivity to GBL decreased from 88% to 38% while the selectivity to BDO increased from 5% to 50% as the hydrogen pressure increased from 3 to 7 MPa. No obvious change was detected in THF selectivity. Such changes in the selectivity revealed the favourable conversion of SA to form GBL over Pd-5FeO_x/C at higher hydrogen pressure.

After each batch of reaction, the representative catalyst (Pd-5FeO_x/C) was recovered and washed with deionized water and then dried at 40°C for the next batch. As shown in Table 3, conversion of SA over fresh Pd-5FeO_x/C catalyst was 54.7% under the reaction condition of 200°C, 5 MPa H_2 and 5 h. Activity of this catalyst decreased gradually with the conversion of SA dropped from 54.7% to 38.9% with no obvious alterations in the product distribution. XRD and TEM results of the used Pd-5FeO_x/C catalyst demonstrated that the size of Pd particles was a little larger than the fresh catalyst (5.4 nm compared to 4.4 nm, Figs. 10 and 11). The ICP-AES analysis of reaction solution showed the leaching of Fe while Pd was quite robust in the reaction media (~5% for Fe and ≤ 0.2% for Pd). The growth of the Pd particles and the leaching of Fe were the main reason for the decay of the catalytic activity.

Biomass-derived SA was also employed in this research to test the feasibility of direct conversion of fermentation SA into BDO and GBL. As for the Pd-5FeO_x/C catalysts, biomass-derived SA hydrogenation displayed a similar variation tendency in products distribution compared to pure commercially available SA. The reaction rate of biomass-derived SA hydrogenation was a little lower than that of pure SA hydrogenation, which may

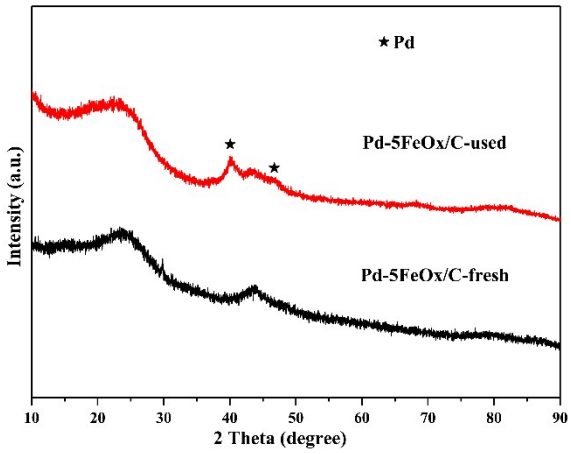

Fig. 10 XRD patterns of the Pd-5FeO_x/C-fresh and the Pd-5FeO_x/C-used catalyst.

Table 3 Reaction results of reusability of Pd-5FeO_x/C catalysts[a]

Recycle run	Conv. (%)	Selectivity (%)				
		THF	GBL	BDO	PA	BA
1	54.7	1.9	83.7	0	3.4	2.8
2	58.5	1.9	84.8	0	3.8	3.0
3	45.8	1.6	84.5	0	4.2	2.6
4	46.5	1.7	85.0	0	3.6	2.5
5	38.9	1.0	83.5	0	4.6	2.3

[a] Reaction conditions: n_{SA}:n_{Pd} = 67:1; T = 200°C; P = 5 MPa H_2 (RT); reaction time = 5 h.
Conv.: conversion, THF: tetrahydrofuran, GBL: γ-butyrolactone, BDO: 1,4-butanediol, PA: propionic acid and BA: butyric acid.

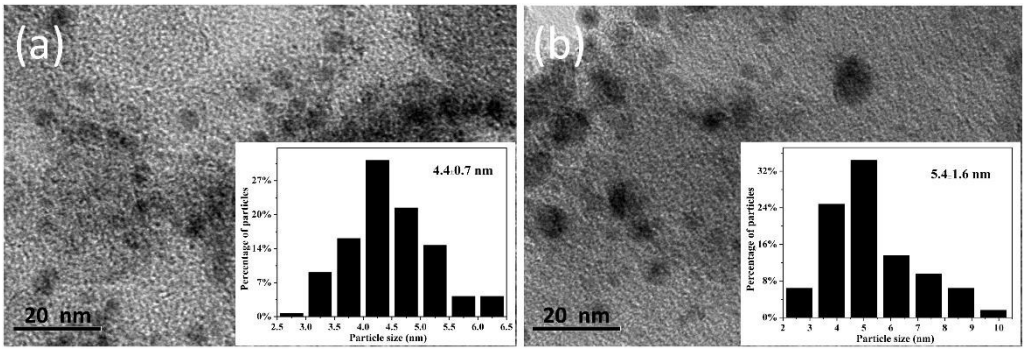

Fig. 11 TEM images of the fresh Pd-5FeO$_x$/C and the used Pd-5FeO$_x$/C catalyst. (a) Pd-5FeO$_x$/C-fresh and (b) Pd-5FeO$_x$/C-used.

result from the residual impurities from fermentation.[18] Conversion of biomass-derived SA was 74% compared to the results of 87% obtained with pure SA as the reactant after 10 h's reaction. A BDO yield of 68% could be obtained with the full conversion of SA under the condition of 200°C, 5 MPa and 60 h. These results indicated that Pd-FeO$_x$/C showed great potential in the direct hydrogenation of biomass-derived SA.

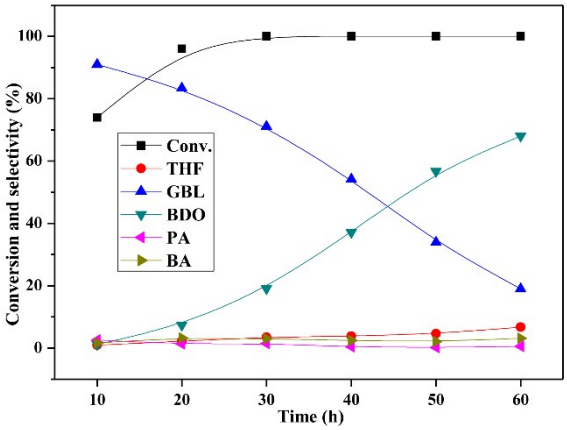

Fig. 12 Hydrogenation of Biomass-derived SA over Pd-5FeO$_x$/C. Reaction conditions: 200°C, 5 MPa H_2, n_{SA}: n_{Pd} = 67:1. THF: tetrahydrofuran, GBL: γ-butyrolactone, BDO: 1,4-butanediol, PA: propionic acid and BA: butyric acid.

Conclusions

In summary, Pd-FeO$_x$/C catalysts are found to be efficient in the aqueous SA hydrogenation to produce GBL, BDO and THF. The addition of Fe not only enhanced the activity of SA conversion, but also promoted the subsequent GBL hydrogenolysis to BDO. Superior activity and the higher selectivity to BDO over Pd-5FeO$_x$/C are ascribed to the high acidity of the catalysts, the well dispersed Pd and the synergy between Pd and Fe species, providing a BDO yield of over 70% under 200°C and 5 MPa H_2. The decrease of catalytic activity in the repeated runs was partially resulted from the relatively poor hydrothermal stability of Pd-FeO$_x$/C catalysts. Further studies are under way to improve the stability of the Pd-FeO$_x$/C catalysts, and to achieve the rational design of catalysts capable of efficient conversion of biomass-derived organic acids to value-added chemicals.

Acknowledgements

This research was supported by grants from the National Natural Science Foundation of China (No. 21273260 and No. 21433001), Shandong Provincial Natural Science Foundation for Distinguished Young Scholar, China (No. JQ201305), "135" Projects Fund of CAS-QIBEBT Director Innovation Foundation and the Chinese Academy of Sciences.

Notes and references

1 A. M. Ruppert, K. Weinberg and R. Palkovits, *Angew. Chem. Int. Ed.,* 2012, **51**, 2564-2601.
2 Y. Nakagawa, M.Tamura and K. Tomishige, *J. Mater. Chem. A,* 2014, **2**, 6688-6702.
3 X. R. Liu, X. C. Wang, S. X. Yao, Y. J. Jiang, J. Guan and X. D. Mu, *RSC Adv.,* 2014, **4**, 49501-49520.
4 D. M. Alonso, S. G. Wettstein and J. A. Dumesic, *Chem. Soc. Rev.,* 2012, **41**, 8075-8098.
5 A. A. Koutinas, A. Vlysidis, D. Pleissner, N. Kopsahelis, I. L. Garcia, I. K. Kookos, S. Papanikolaou, T. H. Kwan and C. S. K. Lin, *Chem. Soc. Rev.,* 2014, **43**, 2587-2627.
6 C. Delhomme, D. Weuster-Botz and F. E. Kühn, *Green Chem.,* 2009, **11**, 13-26.
7 T. A. Werpy, J. E. Holladay and J. F. White, Top value added chemicals from biomass: I. results of screening for potential candidates from sugars and synthesis gas, Pacific Northwest National Laboratory (PNNL), Richland, WA (US), 2004.
8 M. Besson, P. Gallezot and C. Pinel, *Chem. Rev.,* 2014, **114**, 1827-1870.
9 P. Gallezot, *Chem. Soc. Rev.,* 2012, **41**, 1538-1558.
10 U. G. Hong, H. W. Park, J. Lee, S. Hwang and I. K. Song, *J. Ind. Eng. Chem.,* 2012, **18**, 462-468.
11 U. G. Hong, J. Lee, S. Hwang and I. K. Song, *Catal. Lett.,* 2010, **141**, 332-338.
12 B. Tapin, F. Epron, C. Especel, B. K. Ly, C. Pinel and M. Besson, *ACS Catal.,* 2013, **3**, 2327-2335.
13 R. Luque, J. H. Clark, K. Yoshida and P. L. Gai, *Chem. Commun.,* 2009,**35**, 5305-5307.
14 R. M. Deshpande, V. V. Buwa, C. V. Rode, R. V. Chaudhari and P. L. Mills, *Catal. Commun.,* 2002, **3**, 269-274.
15 B. Tapin, F. Epron, C. Especel, B. K. Ly, C. Pinel and M. Besson, *Catal. Today,* 2014, **235**, 127-133.
16 Z. Shao, C. Li, X. Di, Z. Xiao and C. Liang, *Ind. Eng. Chem. Res.,* 2014, **53**, 9638-9645.
17 K. H. Kang, U. G. Hong, Y. Bang, J. H. Choi, J. K. Kim, J. K. Lee, S. J. Han and I. K. Song, *Appl. Catal., A,* 2015, **490**, 153-162.

18 D. P. Minh, M. Besson, C. Pinel, P. Fuertes and C. Petitjean, *Top. Catal.,* 2010, **53**, 1270-1273.
19 K. H. Kang, U. G. Hong, J. O. Jun, J. H. Song, Y. Bang, J. H. Choi, S. J. Han and I. K. Song, *J. Mol. Catal. A: Chem.,* 2014, **395**, 234-242.
20 H. Z. Liu, *Chin. J. Catal.,* 2014, **35**, 1619-1640.
21 S. Abello and D. Montane, *ChemSusChem,* 2011, **4**, 1538-1556.
22 A. A. Adesina, *Appl. Catal., A,* 1996, **138**, 345-367.
23 N. S. Babu, N. Lingaiah, J. V. Kumar and P. S. S. Prasad, *Appl. Catal., A,* 2009, **367**, 70-76.
24 I. A. Witońska, M. J. Walock, M. Binczarski, M. Lesiak, A. V. Stanishevsky and S. Karski, *J. Mol. Catal. A: Chem.,* 2014, **393**, 248-256.
25 X. Niu, J. Gao, Q. Miao, M. Dong, G. Wang, W. Fan, Z. Qin and J. Wang, *Micropor. Mesopor. Mater.,* 2014, **197**, 252-261.
26 X. Lu, L. Luo and X. Chen, *React. Kinet. Catal. Lett.,* 2008, **94**, 35-46.
27 Y. Shu, D. Ma, L. Xu, Y. Xu and X. Bao, *Catal. Let.,* 2000, **70**, 67-73.
28 S. Brandenberger, O. Krocher, A. Wokaun, A. Tissler and R. Althoff, *J. Catal.,* 2009, **268**, 297-306.
29 Y. Wang, Q. H. Zhang, T. Shishido and K. Takehira, *J. Catal.,* 2002, **209**, 186-196.
30 F. Pinna, M. Selva, M. Signoretto, G. Strukul, F. Boccuzzi, A. Benedetti, P. Canton and G. Fagherazzi, *J. Catal.,* 1994, **150**, 356-367.
31 K. N. Rao, B. M. Reddy and S. E. Park, *Appl. Catal. B,* 2010, **100**, 472-480.
32 M. Brun, A. Berthet and J. C. Bertolini, *J. Electron Spec.,* 1999, **104**, 55-60.
33 E. V. Golubina, E. S. Lateva, V. V. Lunin, N. S. Telegina, A. Y. Stakheev and P. Tundo, *Appl. Catal., A,* 2006, **302**, 32-41.
34 F. Rahimi and A. I. Zad, *J. Phys. D Appl. Phys.,* 2007, **40**, 7201-7209.
35 X. L. Du, Q. Y. Bi, Y. M. Liu, Y. Cao, H. Y. He and K. N. Fan, *Green Chem.*, 2012, **14**, 935-939.

Graphical abstract

Pd-FeO_x/C catalysts were prepared and found to be efficient in succinic acid hydrogenation to produce 1,4-butanediol in one-pot.